THE JOURNAL OF BIOLOGICAL CHEMISTRY VOL. 282, NO. 10, pp. 7385–7396, March 9, 2007
Printed in the U.S.A.

Multiple Residues in the Second Extracellular Loop Are Critical for M_3 Muscarinic Acetylcholine Receptor Activation*

Received for publication, November 7, 2006, and in revised form, January 5, 2007 Published, JBC Papers in Press, January 9, 2007, DOI 10.1074/jbc.M610394200

Marco Scarselli[‡], Bo Li[†‡], Soo-Kyung Kim[§1], and Jürgen Wess[‡2]

From the [‡]Molecular Signaling and the [§]Molecular Recognition Sections, Laboratory of Bioorganic Chemistry, NIDDK, National Institutes of Health, Bethesda, Maryland 20892

Recent studies suggest that the second extracellular loop (o2 loop) of bovine rhodopsin and other class I G protein-coupled receptors (GPCRs) targeted by biogenic amine ligands folds deeply into the transmembrane receptor core where the binding of *cis*-retinal and biogenic amine ligands is known to occur. In the past, the potential role of the o2 loop in agonist-dependent activation of biogenic amine GPCRs has not been studied systematically. To address this issue, we used the M_3 muscarinic acetylcholine receptor (M3R), a prototypic class I GPCR, as a model system. Specifically, we subjected the o2 loop of the M3R to random mutagenesis and subsequently applied a novel yeast genetic screen to identity single amino acid substitutions that interfered with M3R function. This screen led to the recovery of about 20 mutant M3Rs containing single amino acid changes in the o2 loop that were inactive in yeast. In contrast, application of the same strategy to the extracellular N-terminal domain of the M3R did not yield any single point mutations that disrupted M3R function. Pharmacological characterization of many of the recovered mutant M3Rs in mammalian cells, complemented by site-directed mutagenesis studies, indicated that the presence of several o2 loop residues is important for efficient agonist-induced M3R activation. Besides the highly conserved Cys^{220} residue, Gln^{207}, Gly^{211}, Arg^{213}, Gly^{218}, Ile^{222}, Phe^{224}, Leu^{225}, and Pro^{228} were found to be of particular functional importance. In general, mutational modification of these residues had little effect on agonist binding affinities. Our findings are therefore consistent with a model in which multiple o2 loop residues are involved in stabilizing the active state of the M3R. Given the high degree of structural homology found among all biogenic amine GPCRs, our findings should be of considerable general relevance.

G protein-coupled receptors (GPCRs)[3] represent the largest class of cell surface receptors found in nature (1–6). GPCR-mediated signaling pathways regulate the activity of an extraordinarily large number of physiological functions. GPCRs are activated by the binding of different structural classes of extracellular ligands, including neurotransmitters, hormones, and sensory stimuli (1–6). All GPCRs are predicted to share a common molecular structure consisting of seven transmembrane helical domains (TM I–VII) connected by three intracellular and three extracellular loops (1–3).

Based on sequence similarity, the mammalian GPCRs can be subclassified into several major subfamilies (1–6). Family I represents by far the largest subgroup of GPCRs, consisting of about 700 different members in human (4). Because the members of this receptor family share considerable sequence homology with rhodopsin, the class I GPCRs are also referred to as rhodopsin-like GPCRs. Most small ligands acting on class I GPCRs, including rhodopsin and the classic biogenic amine ligands such as acetylcholine, dopamine, norepinephrine, or serotonin, are predicted to bind to their target receptors within a cavity formed by the ring-like arrangement of the seven TM helices (7–10). Specifically, these ligands are thought to interact with amino acids located within the exofacial segments of TM III, V, VI, and VII (7–10).

Interestingly, the x-ray structure of bovine rhodopsin suggests that residues contained in the second extracellular loop (o2 loop) may also play a role in ligand (*cis*-retinal) binding, and, perhaps, rhodopsin activation (11). The x-ray structure clearly shows that a portion of the o2 loop, the so-called β4 strand, folds deeply into the center of the TM receptor core, allowing several o2 loop residues to contact the *cis*-retinal ligand (11). In contrast, the two other extracellular loops run along the periphery of the receptor molecule. The proper orientation of the o2 loop is maintained by a disulfide bond that is highly conserved among class I GPCRs (1, 2, 11). One of the Cys residues involved in this disulfide bond is located in the center of the o2 loop (corresponding to Cys^{220} in Fig. 1), and the other one is located at the extracellular end of TM III (corresponding to Cys^{140} in Fig. 1). Numerous studies have shown that the presence of this conserved disulfide bond is critical for proper receptor folding and cell surface localization (see Ref. 12 and references therein).

* This work was supported by the Intramural Research Program of the National Institutes of Health, NIDDK. The costs of publication of this article were defrayed in part by the payment of page charges. This article must therefore be hereby marked "*advertisement*" in accordance with 18 U.S.C. Section 1734 solely to indicate this fact.

† This article is dedicated to the memory of Bo Li who died in a tragic traffic accident on October 20, 2006.

[1] Present address: Beckman Institute, California Institute of Technology, Pasadena, CA 91125.

[2] To whom correspondence should be addressed: Molecular Signaling Section, Laboratory of Bioorganic Chemistry, NIDDK, National Institutes of Health, Bldg. 8A, Rm. B1A-05, 8 Center Dr., MSC 0810, Bethesda, MD 20892-0810. Tel.: 301-402-3589; Fax: 301-480-3447; E-mail: jwess@helix.nih.gov.

[3] The abbreviations used are: GPCR, G protein-coupled receptor; EGFP, enhanced green fluorescent protein; HA tag, hemagglutinin tag; [^{3}H]NMS, *N*-[^{3}H]methylscopolamine; i3 loop, the third intracellular loop of G protein-coupled receptors; M3R, M_3 muscarinic receptor; M3R(Δi3), M_3 muscarinic receptor lacking amino acids Ala^{274}–Lys^{469}; M3RΔ(Nterm), M_3 muscarinic receptor lacking amino acids Thr^2–His^{62}; N-term, the extracellular N-terminal segment of G protein-coupled receptors; o2 loop, the second extracellular loop of G protein-coupled receptors; SC medium, synthetic complete medium; TM I–VII, the seven transmembrane domains of G protein-coupled receptors; GFP, green fluorescent protein; MAPK, mitogen-activated protein kinase; FLIPR, fluorometric imaging plate reader.

Interestingly, biochemical analysis of the D_2 dopamine receptor by the substituted-cysteine accessibility method strongly suggests that the o2 loop of biogenic amine GPCRs may adopt a structure similar to that observed with bovine rhodopsin (13).

At present, little is known about the roles of the extracellular receptor domains in the function of class I GPCRs that are activated by small diffusible ligands. In the case of the muscarinic receptors, the extracellular domains, including the o2 loop, have been shown to play important roles in the binding of certain snake toxins that prevent receptor activation by classic muscarinic agonists (14–16). Moreover, mutagenesis studies carried out with different muscarinic receptor subtypes suggest that residues located within the o2 loop and other extracellular domains make critical contacts with allosteric muscarinic ligands (17). However, it remains unclear whether the o2 loop, or residues contained within other extracellular receptor regions, contributes to the binding of classic muscarinic agonists and/or agonist-induced receptor activation.

To address this issue, we have used the M_3 muscarinic acetylcholine receptor (M3R), a prototypic class I GPCR that is preferentially coupled to G proteins of the G_q family (8), as a model system. In previous studies, we identified many residues located within different TM helices and on the intracellular receptor surface that are critical for various aspects of M3R function (8). Because of the critical role of the o2 loop in ligand recognition in rhodopsin, we decided to investigate whether efficient M3R activation depends on the presence of specific o2 loop residues (besides the conserved Cys^{220} residue). In general, classic mutagenesis techniques are limited by the relatively small number of mutations that can be generated and analyzed in one particular study. We therefore decided to use random mutagenesis techniques to generate a large library of mutant M3Rs containing point mutations in the o2 loop ("o2 loop library"). To select for point mutations that interfere with M3R function, we employed a novel yeast genetic screen that allows the recovery of yeast clones expressing functionally inactive M3Rs (18). In contrast to this approach, previous yeast genetic screens that were used to study GPCR function were all designed to recover functionally active mutants GPCRs (19–26).

As is the case for the o2 loop, the potential functional roles of the N-terminal extracellular domain (N-term) has also not been studied systematically in class I GPCRs. In bovine rhodopsin, the N-term region, together with the o2 loop, forms a compact structure at the entrance of the TM-binding core (11). We therefore also generated an "N-term library" of randomly mutagenized M3Rs and subjected this library to the same genetic screen as described above for the o2 loop library.

Following the initial yeast screen, all receptors harboring single inactivating point mutations were expressed and characterized in more detail in transfected mammalian (COS-7) cells. In addition, we also generated and analyzed (in transfected COS-cells) a series of mutant M3Rs in which specific amino acids in the o2 loop were replaced with alanine (Ala). These Ala substitutions were introduced at sites predicted to be critical for efficient M3R activation, based on the initial characterization of the mutant M3Rs recovered in the yeast genetic screen.

By using this spectrum of complementary experimental approaches, we were able to identify several o2 loop residues that are critical for efficient agonist-induced M3R activation but do not seem to play an important role in the binding of carbachol, a classic muscarinic agonist. The majority of these residues is conserved among all five muscarinic receptor subtypes (M_1–M_5). To our knowledge, this study represents by far the most comprehensive analysis of the functional role of the o2 loop of a class I GPCR activated by a small diffusible ligand. The experimental approach described here should be generally applicable to all GPCRs that can be expressed in yeast in a functional form.

EXPERIMENTAL PROCEDURES

Materials—Carbamylcholine chloride (carbachol), atropine sulfate, and 3-amino-1,2,4-triazole were obtained from Sigma. *N*-[^{3}H]Methylscopolamine ([^{3}H]NMS; 79–83 Ci/mmol) was from PerkinElmer Life Sciences. Media for mammalian cell culture were from Invitrogen. Yeast media components were purchased from Qbiogene. All enzymes used for molecular cloning were from New England Biolabs.

Properties of the Yeast Strain Used and Yeast Growth and Transformation—The haploid yeast (*Saccharomyces cerevisiae*) strain MPY578q5 (*MAT**a** GPA1 far1::LYS2 fus1::FUS1-HIS3 sst2::SST2-G418r ste2::LEU2 fus2::FUS2-CAN1 ura3 lys2 ade2 his3 leu2 trp1 can1*) was used as a host for the expression of all M3R constructs (27). This strain harbors a mutant version of the endogenous *GPA1* gene coding for a modified version of the Gpa1p G protein α subunit in which the last 5 amino acids of Gpa1p were replaced with the corresponding sequence derived from mammalian $G\alpha_q$. Moreover, this strain lacks functional *FAR1*, *SST2*, and *STE2* genes and contains the pheromone-sensitive *FUS1-HIS* and *FUS2-CAN1* reporter genes (Fig. 2). Yeast cells were grown and transformed with plasmid DNA as described previously (24, 27).

Generation of Yeast Libraries Expressing Randomly Mutagenized M3Rs—For yeast expression studies, all mutations were introduced into a modified version of the rat M3R lacking the central portion of the i3 loop (Ala^{274}–Lys^{469}) and containing an N-terminal hemagglutinin (HA) and a C-terminal enhanced green fluorescent protein (EGFP) tag (Fig. 1) (18). For the sake of simplicity, this receptor is referred to as M3R(Δi3) throughout. The M3R(Δi3) coding sequence was inserted into the p416GPD yeast expression plasmid as described previously (27), yielding plasmid p416GPD-M3R(Δi3). The M3R(Δi3) sequence coding for the extracellular N-terminal domain of the receptor (Thr^2–Gln^{66}, Fig. 1) was subjected to PCR-based random mutagenesis to generate, on average, one nucleotide misincorporation per receptor construct (28). PCRs were carried out in 50 μl in the presence of 10 mM Tris-HCl (pH 8.3), 50 mM KCl, 7 mM $MgCl_2$, 0.5 mM $MnCl_2$, 0.001% (w/v) gelatin, 1 mM dCTP, 1 mM dTTP, 0.2 mM dATP, 0.2 mM dGTP, 0.5 μM of each primer, 50 ng of template DNA (p416GPD-M3R(Δi3)), and 3 units of AmpliTaq DNA polymerase (Applied Biosystems). PCR cycling conditions were as follows: 35 cycles at 94 °C for 60 s, 55 °C for 60 s, and 72 °C for 60 s. The following PCR primers were used: sense, 5′-TTA GTT TCG ACG GAT TCT AGA ACT AGA AAA ATG TAC CCC

TAC GAC GTC CCC GAC TAC GCC-3′; antisense, 5′-GAT GGT CAC CAA TGC CAG GAA GCC AGT TAA GAA GGC AAT GAA GAC CAC-3′. The size of the final PCR product was 306 bp.

To generate a library of yeast clones expressing mutant M3Rs containing point mutations within the extracellular N-terminal domain, we used a gap-repair protocol (27, 29). The 306-bp PCR fragment (~4 μg) generated under error-prone PCR conditions (see previous paragraph) was cotransformed into MPY578q5 with the p416GPD-M3R(Δi3) yeast expression plasmid (~10 μg) that had been linearized with AatII within the region corresponding to the 306-bp PCR fragment. This procedure resulted in a yeast expression library consisting of ~1 × 10^5 primary transformants (colonies that were able to grow on plates lacking uracil).

Similarly, the o2 loop of the M3R(Δi3) was also subjected to random mutagenesis. In this case, we used an oligonucleotide that had been synthesized chemically under error-prone conditions (30). The following sense primer coding for M3R residues Pro^{201} to Phe^{232} was synthesized by Genemed Synthesis Inc. (San Francisco, CA): 5′-CCT GCC ATC TTG TTC TGG CAA TAC TTT GTA GGG AAG AGA ACT GTG CCC CCA GGA GAA TGT TTC ATT CAG TTT CTG AGT GAG CCC ACC ATC ACC TTC-3′. The underlined sequence, which corresponds to o2 loop residues Phe^{205} to Pro^{228} (Fig. 1), was synthesized under conditions that led to one nucleotide misincorporation (on average) per molecule (the underlined sequence was doped with 1% non-wild-type nucleotides). A standard PCR was then carried out using this mutagenic sense primer together with an antisense primer (5′-GGC GGC CTT CTT CTC CTT GAT GAG-3′; corresponding to residues Leu^{482} to Ala^{489}) to generate a PCR product of 246 bp. This 246-bp PCR fragment was then used as a template for a second round of PCR using a sense primer that overlapped with the first 12 nucleotides (underlined) of the mutagenic oligonucleotide (5′-ATG ATT GGT CTG GCT TGG GTC ATC TCC TTT GTC CTA TGG GCT CCT GCC ATC TTG-3′). The antisense primer was identical to the one used of the first PCR. The resulting 288-bp PCR product (~3 μg) was cotransformed into MPY578q5 with the p416GPD-M3R(Δi3) yeast expression plasmid (~12 μg) linearized with BstXI within the region corresponding to the 288-bp PCR fragment. This gap repair protocol (29) yielded a yeast expression library consisting of ~1 × 10^5 primary transformants (colonies that were able to grow on plates lacking uracil).

Yeast Genetic Screen to Identify Functionally Inactive Mutant M3Rs—As described in the previous paragraph, the primary yeast transformants were grown on plates containing uracil-deficient synthetic complete (SC) medium to select for Ura+ (plasmid-containing) transformants (plating density, ~2,000–8,000 clones/150-mm plate). After incubating the plates for 2 days at 30 °C, the resulting colonies were transferred, via replica-plating, onto plates containing SC medium that lacked both uracil and arginine but contained 1 mM carbachol and 150 μg/ml canavanine. In addition, arginine was omitted from the medium because it can compete with canavanine for uptake by the Can1p transporter. A total of ~1 × 10^5 yeast clones (primary transformants) was screened for each of the two libraries. Yeast clones that survived the carbachol/canavanine selection step were first studied for GFP fluorescence using the FlexStation (excitation wavelength, 485 nm; emission wavelength, 525 nm; Molecular Devices) and epi-fluorescence microscopy (AX10, Carl Zeiss). To quantitate GFP fluorescence via the use of the FlexStation, yeast cell suspensions were analyzed in a 100- μl volume using a 96-wellplate format (Fig. 3). Yeast clones that failed to display pronounced GFP fluorescence were eliminated at this step. The remaining yeast clones were subjected to a second round of screening. Specifically, plasmids were isolated from these clones, amplified in *Escherichia coli* (DH5α), and retransformed into MPY578q5 to confirm the plasmid linkage of the observed growth phenotype.

Expression of Mutant M3Rs Recovered in the Yeast Genetic Screen in Mammalian Cells—Most inactivating point mutations recovered in the yeast genetic screen were subcloned into a mammalian expression vector (pCD-PS) coding for the full-length M3R containing an N-terminal HA and a C-terminal EGFP tag (18). For the sake of simplicity, this receptor is referred to as "WT" M3R throughout. All resulting receptor constructs were transiently expressed in COS-7 cells (24). For receptor binding studies, COS-7 cells were transfected in 100-mm dishes, as described previously (24). For functional studies, COS-7 cells were seeded into 96-well plates (1.5 × 10^4 cells/well; catalog number 3603, Corning Glass) ~24 h before transfection. Cells were transfected with 100 ng of plasmid DNA per well, using the Lipofectamine Plus kit (Invitrogen). Calcium mobilization assays were carried out 2 days after transfections (see below).

Site-directed Mutagenesis—To introduce Ala substitutions at specific positions of the o2 loop of the "WT" M3R, we used the QuikChange site-directed mutagenesis kit from Stratagene, following the manufacturer's instructions. To generate a mutant "WT" M3R that lacked most of the extracellular N-terminal domain (M3RΔ(Nterm); amino acids Thr^2–His^{62} were deleted), we used standard PCR-based mutagenesis techniques. The identity of all receptor constructs was verified by DNA sequencing.

Radioligand Binding Studies—Transfected COS-7 cells were harvested ~72 h after transfection, and cell membranes were prepared as described in detail previously (24). Radioligand binding assays were carried out in a 1-ml volume using membranes prepared from transfected COS-7 cells suspended in a buffer containing 25 mM sodium phosphate and 5 mM $MgCl_2$ (pH 7.4). Samples were incubated for 3 h at room temperature (22 °C) in the presence of the muscarinic antagonist [^{3}H]NMS. [^{3}H]NMS saturation binding and [^{3}H]NMS/carbachol inhibition binding studies were carried out essentially as described (24). Nonspecific binding was assessed as binding remaining in the presence of 10 μM atropine. Reactions were terminated by rapidly filtration over GF/C Brandel filters, and the amount of bound radioactivity was determined by liquid scintillation spectrometry. Binding data were analyzed using the nonlinear curve-fitting program Prism 4.0b (GraphPad).

Functional Assays (FLIPR)—Functional assays were carried out with receptor-expressing COS-7 cells 2 days after transfection. Specifically, we used FLIPR technology (Molecular Devices) to measure carbachol-mediated increases in intracel-

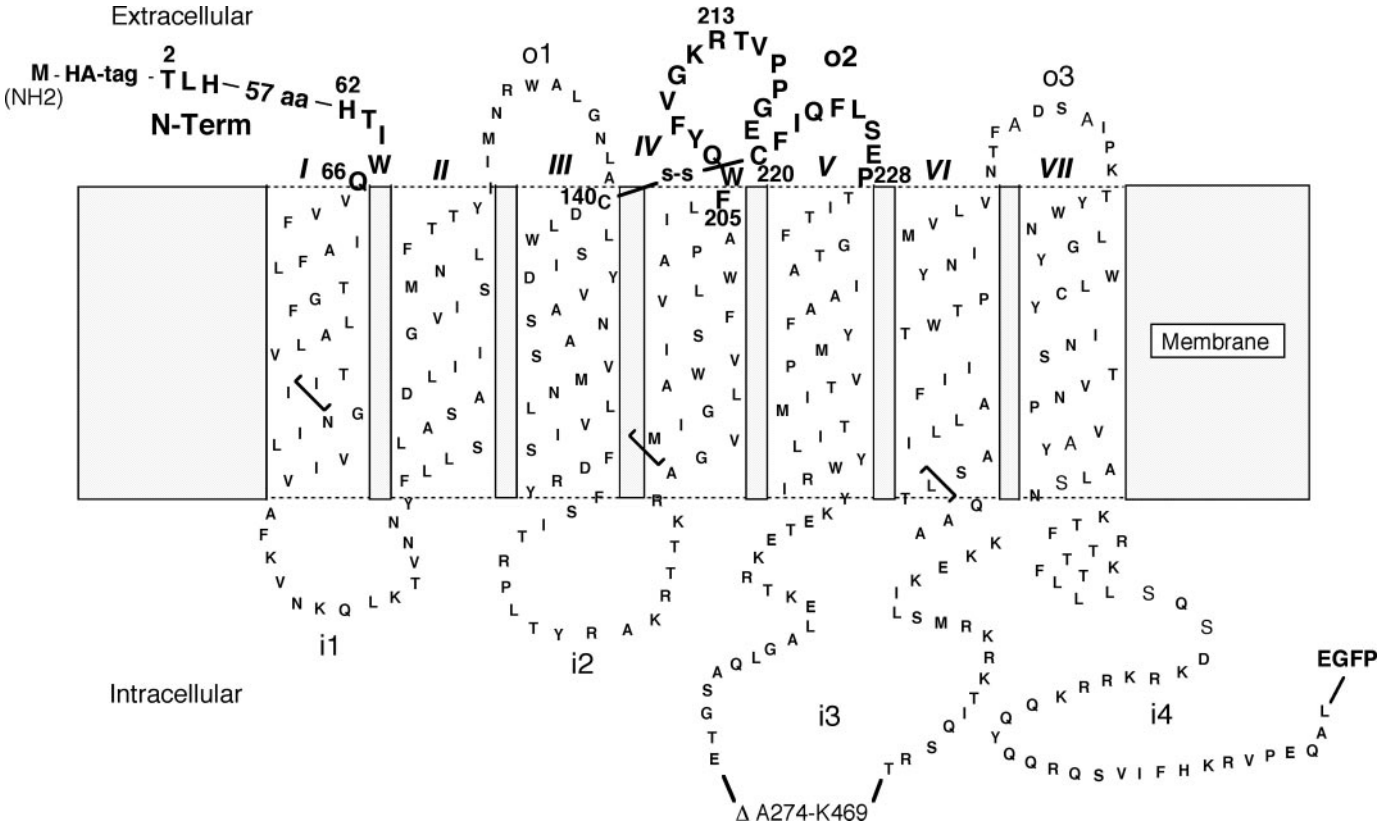

FIGURE 1. **Amino acid sequence of the rat M3R highlighting residues that were targeted in this study.** For expression studies in yeast, all mutations were introduced into a modified version of the rat M3R (M3R(Δi3)) lacking the central portion of the i3 loop (Ala^{274}–Lys^{469}) and containing an HA tag (amino acid sequence, YPYDVPDYA) at the N terminus and an EGFP tag at the C terminus, respectively (18). The extracellular N-terminal region (Thr^{2}–Gln^{66}) and the o2 loop (Phe^{205}–Pro^{228}) were subjected to random mutagenesis. The *brackets* shown correspond to the 3′ and 5′ ends of the PCR products that were produced to generate the two yeast expression libraries (see "Experimental Procedures" for details). Amino acid numbers refer to positions in the full-length rat M3R sequence (46).

lular calcium levels. COS-7 cells grown in 96-well plates were washed once with 200 μl of Hanks' balanced salt solution containing 20 mM HEPES (pH 7.4) and then incubated for 1 h at 37 °C with 30 μl of loading dye (FLIPR Calcium 3 assay kit, Molecular Devices), supplemented with 5 mM probenecid to increase dye retention. Subsequently, increasing concentrations of carbachol were added, and changes in cell fluorescence were measured at room temperature via FLIPR (FLIPR TETRA, Molecular Devices; excitation wavelength, 470 – 495 nm; emission wavelength, 515–575 nm), as described previously (31). For each carbachol concentration, increases in intracellular calcium levels were measured as peak fluorescence activity (FI) minus basal FI prior to the addition of carbachol. Carbachol E_{max} and EC_{50} values were obtained from concentration-response curves using GraphPad Prism (version 4.0b; GraphPad Software). To normalize the functional data obtained with the different mutant M3R constructs, "WT" M3R-expressing cells were included in each individual experiment. In all experiments, the E_{max} value obtained with "WT" M3R-expressing cells was set equal to 100%. Assays were carried out in quadruplicate.

Receptor Modeling—A three-dimensional model of the TM core of the rat M3R, including the various loop regions and helix 8, was built using homology modeling based on the x-ray structure of the inactive state of bovine rhodopsin (11), as described previously (48). To model the o2 loop of the M3R, the two β-sheet domains (β3 and β4) of the o2 loop of bovine rhodopsin were first aligned with the corresponding M3R sequences, followed by the addition or deletion of specific o2 loop segments.

Data Analysis—Binding and functional parameters were estimated using Prism, version 4.0b (GraphPad Software). Carbachol IC_{50} values determined in [^{3}H]NMS/carbachol inhibition binding studies were converted to K_i values by using the Cheng-Prusoff equation (32).

RESULTS

Identification of Single Point Mutations in the o2 Loop That Abolish M3R Function in Yeast—In this study, we used random mutagenesis to introduce point mutations into the extracellular N-terminal region (N-term) and the o2 loop of the rat M3R. All mutations were introduced into a modified version of the M3R that lacked the central portion of the third intracellular loop (i3 loop; Ala^{274}–Lys^{469}) and contained an N-terminal HA and a C-terminal EGFP tag (Fig. 1). For the sake of simplicity, this construct is referred to as M3R(Δi3) throughout. We recently demonstrated that the N- and C-terminal tags do not interfere with M3R function in yeast and mammalian cells (18). Moreover, the deletion of residues Ala^{274}–Lys^{469} leads to a dramatic improvement of M3R expression levels in yeast (27), but it has no significant effect on the ligand binding and G protein-coupling properties of the M3R (12, 33, 34).

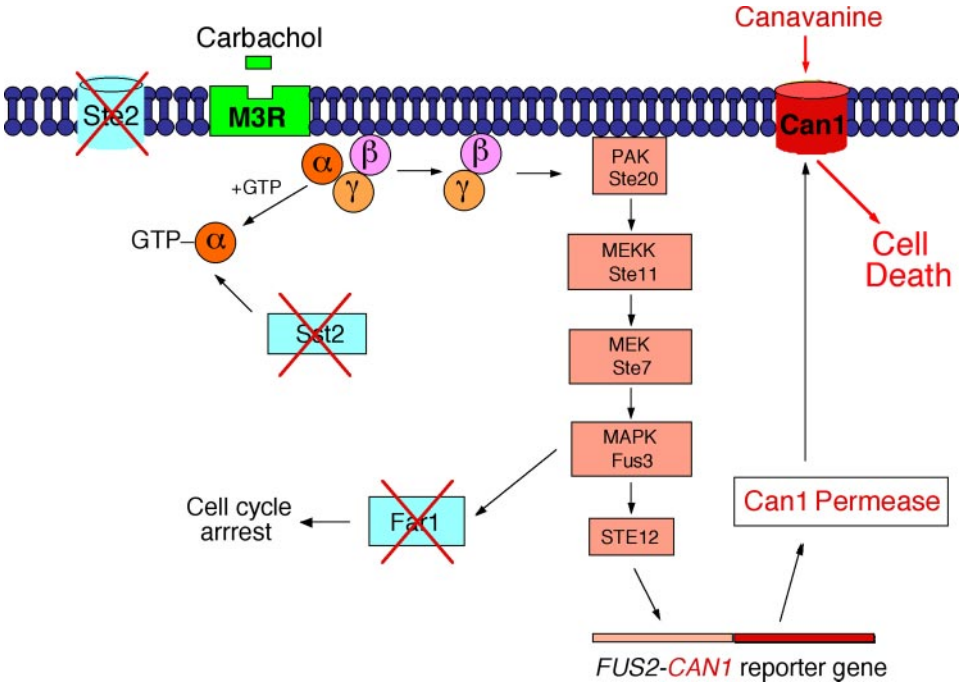

FIGURE 2. **Summary of the yeast pathway linking carbachol-mediated M3R activation to cell death.** All M3R constructs were expressed in the MPY578q5 yeast (*S. cerevisiae*) strain. This strain has been subjected to the following genetic manipulations (27, 47) allowing the recovery of inactive mutant M3Rs under appropriate selection conditions (see below) as follows. 1) The endogenous yeast pheromone GPCR gene (*STE2*) has been deleted. 2) The endogenous G protein α subunit (Gpa1p) has been substituted with a chimeric yeast/mammalian Gα protein in which the last five amino acids of Gpa1p were replaced with the corresponding residues present in mammalian Gα_q. 3) The *SST2* gene ,which codes for an RGS protein, has been deleted to increase the lifetime of the activated G protein. 4) The *FAR1* gene has been deleted to permit yeast growth despite activation of the MAPK pathway. In this strain, carbachol binding to functional M3Rs leads to the activation of the yeast MAPK/pheromone pathway. Stimulation of this pathway eventually leads to activation of the pheromone-sensitive *FUS2-CAN1* reporter gene and the expression of Can1 permease that acts as a transporter protein for the cytotoxic agent canavanine. Thus, yeast clones that express functional M3Rs will not grow in the simultaneous presence of carbachol and canavanine. However, under the same experimental conditions, yeast clones containing functionally inactive mutant M3Rs will give rise to colonies from which plasmid DNAs can be isolated and sequenced.

The M3R(Δi3) construct and all M3R(Δi3)-derived mutant receptors were expressed in the MPY578q5 yeast (*S. cerevisiae*) strain (27). Besides containing several other genetic modifications (see Fig. 2 and "Experimental Procedures" for details), this strain expresses a chimeric yeast Gpa1p/mammalian Gα_q G protein α subunit in which the last five amino acids of Gpa1p were replaced with the corresponding mammalian Gα_q residues. When expressed in the MPY578q5 strain, the M3R(Δi3) is able to activate this chimeric G protein with high efficiency, leading to the stimulation of the yeast pheromone pathway which in turn triggers the activation of the pheromone-sensitive *FUS2-CAN1* receptor gene (18, 27) (Fig. 2).

We subjected the N-term region (Thr^2–Gln^{66}) and the o2 loop (Phe^{205}–Pro^{228}) of the M3R(Δi3) to PCR/oligonucleotide-based random mutagenesis (see "Experimental Procedures" for details). PCR products containing nucleotide misincorporations were cotransformed into MPY578q5 with a gapped (linearized) version of the M3R(Δi3)-p416GPD yeast expression plasmid. This procedure, also referred to as the gap-repair method (29), led to the regeneration of circular plasmids, because of the high recombination activity of yeast.

To generate a large number of mutant receptors containing single amino acid substitutions and to reduce the likelihood of generating receptor constructs harboring multiple amino acid changes, we chose mutagenic conditions that led to a rather low mutagenesis rate (0.5–1 nucleotide changes per receptor construct). To assess the quality of the N-term and o2 loop yeast libraries, we recovered and sequenced plasmids from 60 randomly picked yeast colonies (primary transformants; 30 colonies from each library) growing on plates containing SC medium lacking uracil (SC-Ura medium; note that the p416GPD plasmid contains the URA selection marker). This analysis showed that the nucleotide misincorporation rate for the N-term library was ~0.7 nucleotides per receptor construct. A similar mutagenesis rate was found for the o2 loop library (~0.9 nucleotides per receptor construct). We noted that the nucleotide changes were randomly distributed throughout the two targeted receptor sequences.

Altogether, 89 amino acids (Thr^2–Gln^{66} and Phe^{205}–Pro^{228}), corresponding to 267 nucleotides, were subjected to random mutagenesis. The total number of possible single nucleotide changes is 801 (3 × 267). Sequencing studies showed that ~20% of all primary yeast transformants harbored M3R plasmids containing single nucleotide changes. Assuming that the point mutations occurred in a completely random fashion, 4,005 yeast clones should provide a 1× coverage of all possible single nucleotide substitutions (100/20 × 801). As indicated below, we screened a total of ~2×10^5 yeast clones. This number represents an ~50-fold excess over the number required to achieve complete coverage of all possible single nucleotide substitutions. It is therefore highly likely that the number of yeast clones screened in this study included all possible single nucleotide substitutions.

Each yeast library consisted of about 1×10^5 primary transformants giving rise to colonies on SC-Ura medium (plating density, ~2,000–8,000 colonies/150-mm plate). The primary transformants were replica-plated onto SC medium containing carbachol (1 mM) and the cytotoxin canavanine (150 μg/ml) but lacking uracil and arginine (SC-Arg-Ura medium). Arginine was omitted from the medium because it competes with canavanine for uptake by the Can1p transporter. Under these selection conditions, the binding of carbachol to a functional receptor leads to the activation of the *FUS2-CAN1* receptor gene, triggering the synthesis and membrane insertion of the Can1p transporter protein through which the cytotoxin canavanine can enter the yeast cytoplasm (Figs. 2 and 3). As a result, yeast cells expressing functional M3Rs are unable to grow in the presence of carba-

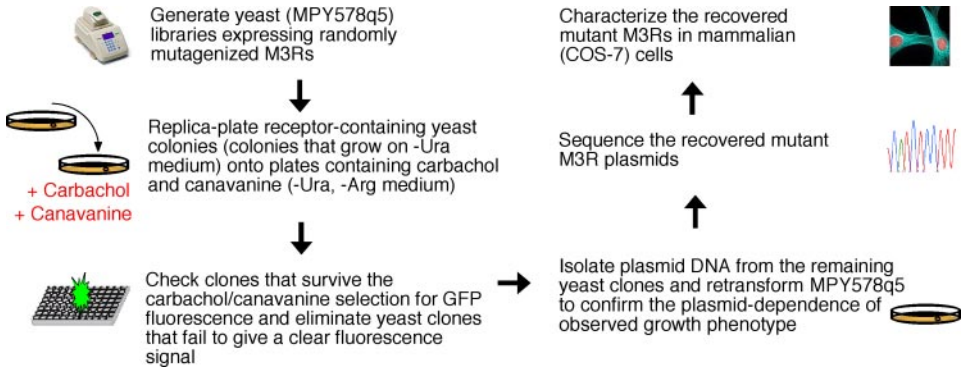

FIGURE 3. **Summary of the strategy used to identify and characterize full-length mutant M3Rs containing inactivating point mutations.** We generated PCR fragments in which the sequences corresponding to the N-terminal region and the o2 loop of the M3R were subjected to random mutagenesis (see "Experimental Procedures" for details). All mutations were introduced into the M3R(Δi3)-p416GPD yeast expression plasmid (Ura selection), taking advantage of the gap-repair method (29). The mutant M3R expression libraries were created using the MPY578q5 yeast strain (see Fig. 2). The primary yeast transformants were replica-plated onto medium that lacked uracil and arginine (SC-Ura-Arg) but contained the cytotoxin canavanine (150 μg/ml) and the muscarinic agonist carbachol (1 mM). Under these conditions, only those yeast clones that contained inactive mutant M3Rs gave rise to colonies. To ensure that the yeast clones that survived the carbachol/canavanine selection procedure contained full-length receptors that were stable in yeast, all surviving clones were studied for GFP fluorescence. Yeast clones that did not yield a robust fluorescence signal were eliminated. Yeast clones displaying robust GFP fluorescence were subjected to a second round of screening. Specifically, plasmids were isolated from these yeast clones, amplified in *E. coli* (DH5α), and retransformed into MPY578q5 to confirm that the observed growth phenotype was indeed plasmid-dependent.

TABLE 1

Single point mutations that disrupted M3R function in yeast

The indicated point mutations disrupted M3R function in yeast strain MPY578q5. Plasmids coding for the indicated mutant receptors were isolated from yeast clones that were able to grow on plates containing carbachol (1 mM) and canavanine (150 μg/ml). All mutations were introduced into the M3R(Δi3) construct, a modified version of the rat M3R that lacked amino acids Ala^{274}–Lys^{469}, and contained an N-terminal HA and a C-terminal EGFP tag (Fig. 1). Yeast clones expressing the indicated mutant receptors showed pronounced GFP fluorescence, indicating that the various point mutations did not destabilize the M3R(Δi3) protein. For details, see "Experimental Procedures."

Inactivating point mutation	No. of recovered yeast clones	Localization
W192C	3	TM IV
S195F	2	TM IV
W199C	2	TM IV
W199R	4	TM IV
P201L	1	TM IV
F205V	1	TM IV/o2 junction
Q207L	4	o2
G211W	2	o2
R213T	4	o2
R213I	3	o2
R213S	4	o2
R213G	2	o2
G218V	1	o2
C220S	6	o2
C220W	3	o2
C220F	4	o2
C220G	4	o2
C220R	2	o2
I222T	3	o2
Q223K	3	o2
Q223L	1	o2
Q223H	2	o2
F224Y	1	o2
F224S	2	o2
F224V	2	o2
L225P	3	o2
P228L	3	o2
F239L	3	TM V
P242S	2	TM V

chol and canavanine. However, under the same experimental conditions, yeast clones harboring functionally inactive mutant M3Rs are able to grow (Figs. 2 and 3).

Altogether, we picked 1,506 (N-term library) and 1,727 yeast colonies (o2 loop library), respectively, that showed robust growth in the presence of carbachol and canavanine. Because the GFP tag was fused to the C terminus of the M3R, mutant receptors containing nonsense mutations (premature stop codons) were predicted to give no GFP signal. Similarly, cells harboring mutant M3Rs that were expressed at low levels in yeast were expected to show only weak GFP fluorescence. To select for full-length mutant receptors that were expressed at high levels in yeast, we therefore examined suspensions of the recovered yeast clones for GFP fluorescence, using a 96-well plate format (see "Experimental Procedures" for details; Fig. 3). Under these experimental conditions, the majority of the analyzed yeast clones showed none or only weak GFP fluorescence. Most likely, these clones contained truncated receptors, either due to nonsense or frameshift mutations, or full-length mutant receptors that were unstable in yeast. However, 372 (~10%) of the analyzed yeast clones gave a robust fluorescence signal. These clones were then subjected to a second round of screening to confirm the plasmid dependence of the growth phenotype. The plasmids contained in the yeast clones that passed this second round of screening (~95%) were sequenced.

Specifically, we sequenced 230 plasmids originating from the o2 loop library. More than half of these plasmids contained multiple point mutations; the encoded mutant receptors were not analyzed further. However, we also identified 77 plasmids coding for mutant M3Rs containing single amino acid changes (Table 1). Most of these single amino acid substitutions were recovered two or more times (Table 1), suggesting that the yeast screen was performed at or near saturating conditions. In several cases, specific o2 loop residues (Arg^{213}, Cys^{220}, Gln^{223}, and Phe^{224}) were found to be replaced by three or more different amino acids (Table 1), indicative of the potential functional importance of these amino acids. We also identified several inactivating point mutations in TM IV and TM V, which are connected by the o2 loop (W192C, S195F, W199C, W199R, P201L, F239L, and P242S; Table 1). Although the TM regions were not targeted by random mutagenesis, it is likely that these mutations arose because of PCR errors during the generation of the PCR fragment used for constructing the o2 loop yeast expression library (see "Experimental Procedures" for details). The W192C, P201L, and P242S point mutations involve three residues that are highly conserved among class I GPCRs (positions 4.50, 4.59, and 5.50 according to the Ballesteros/Weinstein amino acid nomenclature of GPCRs see Ref. 35). The critical functional roles of these amino acids have been documented in a large number of mutagenesis studies, con-

TABLE 2

Characterization of mutant M3Rs recovered in the yeast screen in mammalian cells

The indicated mutant M3Rs were transiently expressed in COS-7 cells. All point mutations were introduced into the "WT" M3R (full-length rat M3R containing an N-terminal HA and a C-terminal EGFP tag). The M3RΔ(Nterm) construct lacks the extracellular N-terminal portion of the M3R (Thr^2–His^{62}; see Fig. 1). The B_{max} value for the "WT" M3R was 4.2 ± 0.7 pmol/mg protein, as determined in [^{3}H]NMS saturation binding studies. Carbachol-mediated increases in intracellular calcium levels were determined via FLIPR, as described under "Experimental Procedures." Data are given as means ± S.E. of three independent experiments.

Receptor	Ligand binding studies			Functional studies	
	[^{3}H]NMS K_d	Carbachol K_i	[^{3}H]NMS B_{max}	Carbachol EC_{50}	Carbachol E_{max}
	pM	μM	%	nM	%
"WT" M3R	106 ± 12	17.2 ± 1.8	100	31.4 ± 7.3	100
Q207L	1,780 ± 44	42.4 ± 6.7	40.2 ± 5.6	18,810 ± 976	60.2 ± 12.3
G211W	184 ± 15	20.3 ± 3.8	28.4 ± 2.6	562 ± 38	71.3 ± 9.3
R213T	488 ± 21	37.2 ± 1.5	35.2 ± 3.4	845 ± 26	82.3 ± 9.1
R213I	475 ± 17	31.6 ± 4.2	30.4 ± 3.5	753 ± 35	77.8 ± 6.2
R213S	135 ± 14	32.1 ± 2.3	38.1 ± 4.8	650 ± 18	80.3 ± 8.3
R213G	231 ± 11	44.5 ± 2.9	39.2 ± 5.6	948 ± 23	85.0 ± 7.4
G218V	118 ± 14	13.2 ± 2.8	36.8 ± 4.2	254 ± 19	94.2 ± 8.0
I222T	166 ± 18	90.2 ± 7.8	65.5 ± 6.3	1,070 ± 37	71.2 ± 7.3
Q223K	566 ± 18	92.4 ± 17.4	58.4 ± 7.4	878 ± 65	94.3 ± 9.1
F224Y	221 ± 15	406 ± 24	56.4 ± 7.5	635 ± 12	88.2 ± 6.6
L225P	510 ± 23	536 ± 25	41.3 ± 5.4	79,390 ± 1,370	71.1 ± 7.6
P228L	169 ± 16	23.4 ± 3.7	30.4 ± 3.5	1,200 ± 99	66.9 ± 8.0
M3RΔ(Nterm)	135 ± 16	13.0 ± 2.8	12.2 ± 1.3	81.4 ± 8.4	40.6 ± 4.5

firming the usefulness of the yeast screening strategy used in this study to identify residues critical for M3R function.

We also sequenced 124 plasmids originating from yeast clones contained in the N-term (Thr^2–Gln^{66}) library that survived the carbachol/canavanine and GFP screening procedures. Most of these plasmids contained multiple point mutations. We did not recover any plasmids coding for receptors harboring single amino acid changes.

Analysis of Inactive Mutant M3Rs Recovered in the Yeast Genetic Screen in Mammalian Cells—Above, we described single point mutations in the o2 loop that abolished M3R activity in yeast. We next wanted to explore whether these mutations had similar effects in a mammalian expression system. Toward this goal, we introduced representative point mutations into a mammalian expression plasmid (pCD) coding for the full-length M3R containing an N-terminal HA and a C-terminal EGFP tag. For the sake of simplicity, this receptor construct is referred to as "WT" M3R throughout. We recently reported that the N- and C-terminal tags have little effect on the ligand binding and functional properties of the M3R (18).

The "WT" M3R and all "WT" M3R-derived mutant receptors were transiently expressed in COS-7 cells and characterized in radioligand binding and functional studies (Table 2). In a previous study, we demonstrated that Cys^{220} plays a critical role in proper M3R folding (12). This Cys residue is highly conserved among class I GPCRs and is predicted to form a disulfide bond with a conserved Cys residue present at the extracellular end of TM III (Cys^{140} in the M3R; Fig. 1) (11, 36). Because of this earlier report (12), we did not analyze the recovered Cys^{220} mutant receptors any further (Table 1).

We first studied the ability of the "WT" M3R and the different mutant receptors to bind the muscarinic antagonist [^{3}H]NMS. With the exception of the Q207L construct, all analyzed receptors containing single point mutations in the o2 loop retained the ability to bind [^{3}H]NMS with high affinity (range of K_d values, 118–566 pM; see Table 2). The Q207L mutant receptor bound [^{3}H]NMS with ~17-fold lower affinity, as compared with the "WT" M3R (Table 2). All mutant receptors displayed a reduction in B_{max} values (maximum number of [^{3}H]NMS binding sites), ranging from 28.4 to 65.5% of the corresponding "WT" M3R value (100%; Table 2). [^{3}H]NMS/carbachol inhibition binding studies showed that most analyzed mutant receptors retained the ability to bind the muscarinic agonist, carbachol, with high affinities that differed from the corresponding "WT" M3R value by less than 3-fold (Table 2). However, the I222T, Q223K, F224Y, and L225P mutant receptors showed 5.2-, 5.4-, 24-, and 31-fold, respectively, lower carbachol affinities than the "WT" M3R (Table 2).

To examine whether the different mutant receptors were able to couple to G proteins in transfected COS-7 cells, we measured carbachol-mediated increases in intracellular calcium levels using FLIPR technology. As shown in Table 2, all analyzed mutant receptors retained the ability to trigger carbachol-dependent elevations in intracellular calcium levels. However, with the exception of the Q223K mutant receptor that showed unchanged functional efficacy, all mutant receptors showed a significant reduction in maximum functional responses (E_{max} values), as compared with the "WT" M3R (Table 2). Interestingly, all analyzed mutant receptors showed a pronounced reduction in carbachol potencies (increases in EC_{50} values; Table 2). Although most mutant receptors showed 8–38-fold lower carbachol potencies than the "WT" M3R, the Q207L and the L225P constructs displayed even more dramatic decreases in carbachol potencies (600- and 2,530-fold, respectively; Table 2).

To investigate to which extent the observed decreases in receptor expression levels (B_{max} values) contributed to the functional deficits displayed by the analyzed mutant receptors, we systematically reduced the expression levels of the "WT" M3R and then studied carbachol-mediated calcium responses at different "WT" M3R densities. These studies showed that stepwise reduction of "WT" M3R expression levels led to a progressive decrease in carbachol E_{max} values (Table 3). However, even a drastic reduction in B_{max} values by 80% still yielded an E_{max} value of 48.8% (Table 3, bottom line). In contrast, the stepwise reduction of "WT" M3R expression levels had little effect on carbachol EC_{50} values (Table 3). The maximum reduction in carbachol potency that we observed was only 2.2-fold (Table 3,

bottom line), indicating that under the experimental conditions of the FLIPR assay carbachol potencies were relatively insensitive to changes in receptor B_{max} values. These observations strongly suggest that the pronounced reductions in carbachol potencies displayed by all analyzed mutant receptors are indicative of impaired receptor function, rather than being caused primarily by reduced receptor densities.

As described above, the screening of the N-term yeast expression library failed to yield any receptors containing single amino acid substitutions that disrupted M3R function in yeast. This observation suggested that the extracellular N-terminal domain may not be critical for M3R function. To address this issue in a more direct fashion, we generated a mutant M3R, referred to as M3RΔ(Nterm), that lacked most of the extracellular N-terminal domain (amino acids Thr-2-His-62 were deleted) but still contained the HA epitope tag after the initiating Met codon (Fig. 1). When transiently expressed in COS-7 cells, the M3RΔ(Nterm) construct showed [^{3}H]NMS and carbachol binding affinities similar to the "WT" M3R (Table 2). However, the M3RΔ(Nterm) receptor showed pronounced reductions in B_{max} (by ~90%) and E_{max} values (by ~60%), as compared with the "WT" M3R (Table 2). On the other hand, the M3RΔ(Nterm) construct showed only a small reduction (2.6-fold) in carbachol potency (Table 2). When expressed at similarly low levels (see Table 3, bottom line), the "WT" M3R displayed carbachol EC_{50} and E_{max} values that were similar to those observed with the M3RΔ(Nterm) receptor. This observation strongly suggests that the extracellular N-terminal domain of the M3R does not play an important role in the efficiency of carbachol-mediated receptor activation.

Analysis of Mutant M3Rs Containing Ala Substitutions in the o2 Loop in Mammalian Cells—The yeast genetic screen described above yielded several mutant M3Rs containing single point mutations that showed significant functional deficits in mammalian cells. To examine to which extent these functional impairments were dependent on the chemical nature of the newly introduced amino acid side chains, we generated a series of mutant "WT" M3Rs containing single Ala substitutions at functionally critical o2 loop positions, as predicted by the data shown in Tables 1 and 2. We focused on seven o2 loop residues, mutational modification of which resulted in the most produced reductions in functional carbachol potencies (Table 2). Specifically, the following mutant M3Rs were generated and characterized in transfected COS-7 cells: Q207A, R213A, I222A, Q223A, F224A, L225A, and P228A. In addition, we also included the E219A mutant receptor in this analysis. Although the yeast genetic screen did not lead to the recovery of any amino acid substitutions at this position, we decided to study this mutant receptor because Glu^{219} is the only negatively charged residue present in the o2 loop of the M3R. Because this residue is situated directly adjacent to Cys^{220}, the Glu^{219} side chain is likely to be located inside the TM receptor core (11).

All Ala mutant receptors showed [^{3}H]NMS binding affinities similar to the corresponding "WT" M3R value (Table 4). Moreover, the carbachol binding affinities of all analyzed Ala mutant receptors were either similar to the corresponding "WT" M3R value or differed from this value by less than 5-fold (Table 4). Except for the Q223A construct, all mutant receptors showed a slight reduction in B_{max} values (by ~15–30%; Table 4). In functional assays, three of the analyzed mutant receptors, Q207A, E219A, and Q223A, showed unchanged maximum functional responses to carbachol (E_{max}; Table 4). The remaining mutant receptors showed an ~10–20% reduction in E_{max} values (Table 4). Two of the analyzed mutant receptors, E219A and Q223A, showed similar carbachol potencies as the "WT" M3R (Table 4). Interestingly, however, all remaining Ala mutant receptors (Q207A, R213A, I222A, F224A, L225A, and P228A) displayed

TABLE 3

Effect of M3R expression levels on carbachol-mediated increases in intracellular calcium levels in transfected COS-7 cells

To systematically reduce "WT" M3R expression levels, COS-7 cells were transiently transfected in 100-mm dishes with decreasing amounts of "WT" M3R plasmid DNA (2 (= 100%), 1, 0.5, 0.25, 0.12, or 0.06 μg). B_{max} values were determined in [^{3}H]NMS saturation binding studies, as described under "Experimental Procedures." Carbachol-mediated increases in intracellular calcium levels were measured via FLIPR (for details, see "Experimental Procedures"). Data are given as means ± S.E. of three independent experiments.

"WT" M3R[a] expression level (B_{max})	Carbachol EC_{50}	Carbachol E_{max}
%	nM	%
100	31.4 ± 7.3	100%
89	34.4 ± 5.3	98.0 ± 4.5
65	43.4 ± 7.2	90.5 ± 6.6
46	38.8 ± 3.9	75.4 ± 6.5
29	50.3 ± 4.5	56.1 ± 7.1
20	68.4 ± 6.1	48.8 ± 9.2

[a] The "WT" M3R corresponds to the full-length rat M3R containing an N-terminal HA and a C-terminal EGFP tag.

TABLE 4

Characterization of mutant M3Rs containing Ala substitutions in the o2 loop in mammalian cells

All Ala substitutions were introduced into the 'WT' M3R (full-length rat M3R containing an N-terminal HA and a C-terminal EGFP tag). The indicated receptor constructs were transiently expressed in COS-7 cells and characterized in radioligand binding and functional studies, as described under "Experimental Procedures." The B_{max} value calculated for the 'WT' M3R was 4.2 ± 0.7 pmol/mg protein, as determined in [^{3}H]NMS saturation binding studies. Carbachol-mediated increases in intracellular calcium levels were measured via FLIPR (for details, see "Experimental Procedures"). Data are given as means ± S.E. of three independent experiments.

Receptor	Ligand binding studies			Functional studies	
	[^{3}H]NMS K_d	Carbachol K_i	[^{3}H]NMS B_{max}	Carbachol EC_{50}	Carbachol E_{max}
	pM	μM	%	nM	%
'WT' M3R	106 ± 12	17.2 ± 1.8	100	31.4 ± 7.3	100
Q207A	90.3 ± 7.8	17.0 ± 2.8	78.2 ± 11.3	245 ± 24	102 ± 5
R213A	114 ± 6	34.7 ± 6.1	69.5 ± 9.4	608 ± 22	79.5 ± 6.6
E219A	125 ± 14	25.1 ± 4.2	76.6 ± 7.3	37.1 ± 8.1	101 ± 4
I222A	175 ± 14	72.7 ± 6.5	82.5 ± 8.0	312 ± 19	89.2 ± 5.2
Q223A	111 ± 15	14.2 ± 1.5	97.3 ± 7.0	35.4 ± 8.2	96.0 ± 8.2
F224A	101 ± 9	51.7 ± 4.9	80.1 ± 8.4	239 ± 17	86.2 ± 7.2
L225A	241 ± 10	87.5 ± 9.8	84.6 ± 10.4	403 ± 40	85.4 ± 6.5
P228A	98.4 ± 7.2	50.0 ± 7.2	71.4 ± 8.3	597 ± 44	80.0 ± 7.1

pronounced reductions in carbachol potencies, ranging from 8- to 19-fold, as compared with the "WT" M3R (Table 4).

DISCUSSION

The high resolution x-ray structure of bovine rhodopsin suggests that the extracellular regions of class I GPCRs are highly structured (11). Interestingly, the rhodopsin structure clearly indicates that the o2 loop folds down deeply into the TM receptor core and that several o2 loop residues are in direct contact with the *cis*-retinal ligand (11). A recent biochemical study carried out with Cys-substituted mutant D_2 dopamine receptors suggests that the o2 loop of class I GPCRs that are activated by biogenic amines or other small ligands may share similar structural properties (13). The proper spatial orientation of the o2 loop is maintained by a disulfide bond involving two Cys residues that are highly conserved among class I GPCRs (1, 2. 5, 11, 13). One of the two Cys residues is located in the center of the o2 loop (corresponding to Cys^{220} in the M3R; Fig. 1), and the other one is present at the extracellular end of TM III (corresponding to Cys^{140} in Fig. 1). Site-directed mutagenesis studies with many different class I GPCR subtypes, including the M3R, have shown that this conserved disulfide bond is critical for proper receptor folding and trafficking to the cell surface (see Ref. 12 and references therein).

Besides the extensively studied conserved Cys residue, little is known about the potential functional roles of other amino acids located within the o2 loop. Previous studies have demonstrated that biogenic amines and other small ligands acting on class I GPCRs bind within the TM receptor core by interacting with amino acids located on different TM helices (7–10, 37). For this reason, the potential role of the extracellular receptor domains in agonist-induced activation of class I GPCRs has not been studied systematically. However, because residues in the o2 loop of rhodopsin and biogenic amine receptors are predicted to be located in close proximity of the classic ligand binding pocket (11, 13), it is conceivable that o2 loop residues may play a role in stabilizing the agonist-induced receptor conformation that can productively interact with G proteins.

To test this hypothesis, we initially employed a novel experimental approach that involves receptor random mutagenesis followed by a yeast genetic screen that can recover mutant receptors containing single amino acid substitutions that disrupt receptor function in yeast (18). Using this strategy, we previously identified a large number of single point mutations that abolish M3R function in yeast (18). These mutations were found throughout the M3R coding sequence but occurred with particularly high frequency within the TM receptor core (18). In this study, we used this novel approach to identify mutant M3Rs containing point mutations in the o2 loop and the N-term domain (see below) that disrupt receptor function in yeast. The yeast screen performed by Li *et al.* (18) was carried out under very stringent conditions using a very high concentration of the muscarinic agonist carbachol (10 mM). In this study, we reduced the carbachol concentration to 1 mM, assuming that reducing the stringency of the screen would lead to the recovery of mutant receptors that had not been found previously. The screen by Li *et al.* (18) identified only four inactivating point mutations in the o2 loop (Q207L, C220S, C220R, and L225P), all of which were also recovered in this study (Table 1).

In this study, M3R random mutagenesis was carried out under conditions that favored the generation of mutant receptors containing single amino acid substitutions. Consequently, the receptor libraries that we generated did not contain all possible amino acid changes. However, as has been reviewed recently (38), such libraries nevertheless retain a high level of diversity because multiple amino acid substitutions can still occur at each position.

Screening of the o2 loop library led to the identification of a series of mutant receptors containing single amino acid substitutions that abolished M3R function in yeast (Table 1). Most of these substitutions were recovered multiple times, indicating that the yeast genetic screen was carried out at or near saturating conditions. The recovered point mutations involved the following o2 loop residues: Gln^{207}, Gly^{211}, Arg^{213}, Gly^{218}, Cys^{220}, Ile^{222}, Gln^{223}, Phe^{224}, Leu^{225}, and Pro^{228}. Residues Arg^{213}, Cys^{220}, Gln^{223}, and Phe^{224} were found to be substituted by three or more different amino acids with diverse structural properties (Table 1), suggesting that the side chains of these four o2 loop residues are of particular importance for M3R function.

To examine whether the point mutations recovered in the yeast genetic screen also led to functional deficits in a mammalian expression system, selected mutant receptors that were inactive in yeast were studied in greater detail in transiently transfected COS-7 cells (Table 2). To determine whether the different amino acid substitutions interfered with agonist-dependent G protein activation, we examined carbachol-mediated increases in intracellular calcium levels using FLIPR technology. We found that all analyzed mutant receptors showed pronounced (8–2,530-fold) reductions in carbachol potencies, as compared with the "WT" M3R from which all mutant receptors were derived (Table 2). In contrast, with only few exceptions (see below), the majority of the analyzed o2 loop point mutations had no or only minor effects on carbachol binding affinities (Table 2). Most mutant receptors also displayed significant reductions in receptor expression levels (B_{max}) and carbachol efficacies (E_{max}; Table 2). To study the effects of reduced B_{max} levels on receptor function, we carried out calcium release assays with cells expressing reduced levels of the "WT" M3R (Table 3). This analysis strongly suggested that the pronounced reduction in carbachol EC_{50} values displayed by all analyzed mutant receptors was not primarily a consequence of reduced B_{max} values but was most likely because of mutation-induced impairments in agonist-induced receptor activation.

Interestingly, two of the point mutations recovered in the yeast genetic screen, G211W and G218V, involved the two glycine residues present in the o2 loop of the M3R (Fig. 5). Although the G211W and G218V mutant receptors showed unchanged carbachol binding affinities (as compared with the "WT" M3R), they showed a significant reduction (18- and 8-fold, respectively) in functional carbachol potencies (Table 2). Because glycine residues often function to increase the conformational flexibility of various protein domains (37), one pos-

sibility is that the G211W and G218V mutations impaired receptor function by restricting the conformational freedom of the o2 loop required for efficient M3R activation. Consistent with this concept, biophysical studies suggest that agonist activation of the serotonin 5-$HT_{4(a)}$ receptor involves a rearrangement of the o2 loop (42).

Although all mutant M3Rs listed in Table 1 were inactive in yeast, all analyzed mutant receptors retained considerable activity in transfected COS-7 cells. One possible reason for this phenomenon is that the yeast assay involved the monitoring of yeast growth over a 2-day period, whereas the FLIPR assay used for studying receptor activity in mammalian cells measured fluorescence (calcium) responses that reached maxima within several seconds. Moreover, although the mutant M3Rs were forced to interact with a yeast/mammalian hybrid Gpa1p/α_q G protein in yeast, they were able to couple to native G_q-type G proteins in transfected mammalian cells. Finally, radioligand binding studies have shown that M3Rs are expressed at considerably higher levels (>10-fold) in transfected COS-7 cells than in the MPY578q5 yeast strain (27).

To examine to which extent the newly introduced amino acid side chains contributed to the functional impairment displayed by the mutant M3Rs listed in Table 2, selected o2 loop residues were also subjected to Ala substitution mutagenesis (Table 4). In general, the resulting mutant receptors showed only relatively small or no significant reductions in B_{max} and E_{max} values. However, with only two exceptions, E219A and Q223A, all analyzed Ala mutant receptors (Q207A, R213A, I222A, F224A, L225A, and P228A) showed pronounced reductions (~8–19-fold) in carbachol potencies, as compared with the "WT" M3R (Table 4; Fig. 4). These latter six mutant M3Rs showed either unchanged or only rather small reductions (~2–5-fold) in carbachol binding affinities (Table 4), strongly suggesting that the targeted amino acids are of particular functional importance by enabling carbachol to activate the M3R with high efficiency (potency). The R213A and P228A constructs showed the most pronounced reductions in carbachol potencies (19-fold), suggesting that Arg^{213} and Pro^{228} play key roles in agonist-induced M3R activation.

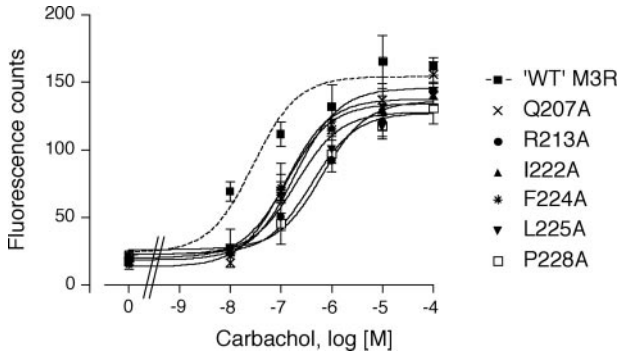

FIGURE 4. **Functional characterization in COS-7 cells of mutant M3Rs in which specific o2 loop residues were replaced with Ala.** All Ala substitutions were introduced into the "WT" M3R. The resulting receptor constructs were transiently expressed in COS-7 cells. Carbachol-induced increases in intracellular calcium levels were measured via FLIPR (for details, see "Experimental Procedures"). Fluorescence counts are given in arbitrary units. The curves shown are representative of three independent experiments. Date are given as means ± S.D. Assays were carried in quadruplicate. Carbachol EC_{50} and E_{max} values are listed in Table 4.

The ligand binding and functional properties of the Q223A mutant receptor were indistinguishable from those of the "WT" M3R (Table 4), suggesting that Gln^{223} does not play a critical role in M3R function. In contrast, the Q223K mutant receptor showed a pronounced reduction (28-fold) in carbachol potency (Table 2). These observations suggest that the functional impairment displayed by the Q223K mutant receptor was most likely because of detrimental structural effects caused by the newly introduced Lys side chain.

Glu^{219} is the only negatively charged residue present in the o2 loop of the M3R (Fig. 5). Moreover, this residue is situated directly adjacent to Cys^{220}, suggesting that Glu^{219} is located inside the TM receptor core (11). Based on these observations, we also analyzed the E219A mutant M3R in transfected COS-7 cells. However, we found that the ligand binding and functional properties of the E219A mutant receptor were similar to those of the "WT" M3R (Table 4), indicating that the presence of Glu^{219} is not required for efficient M3R function. In agreement with this notion, the yeast genetic screen did not lead to the recovery of any mutant M3Rs containing amino acid substitutions at position Glu^{219}.

Fig. 5 shows that the o2 loop residues that are required for efficient agonist-mediated M3R activation (Gln^{207}, Gly^{211}, Arg^{213}, Gly^{218}, Cys^{220}, Ile^{222}, Phe^{224}, Leu^{225}, and Pro^{228}) are scattered throughout the o2 loop sequence. Interestingly, most of these residues (Gln^{207}, Gly^{211}, Arg^{213}, Cys^{220}, Ile^{222}, and Phe^{224}) are conserved among all five muscarinic receptor subtypes (Fig. 5), further highlighting the potential structural and/or functional importance of these residues.

We recently established a three-dimensional model of the inactive state of the M3R, based on homology modeling using the high resolution x-ray structure of bovine rhodopsin as a template (11, 48). Fig. 6 indicates that the functionally critical o2 loop residues identified in this study are located within different o2 loop subdomains (Gln^{207}, beginning of the o2 loop close to TM IV; Gly^{211}, β3 strand; Arg^{213} and Gly^{218}, hinge region connecting the β3 and β4 strands; Cys^{220}, β4 strand; Ile^{222}, Phe^{224}, Leu^{225}, and Pro^{228}, C-terminal segment of the o2 loop).

In a related study, Klco *et al.* (26) subjected the o2 loop of the C5a receptor, another class I GPCR, to random mutagenesis and used a

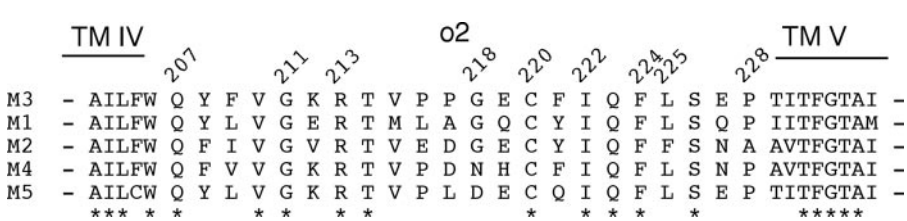

FIGURE 5. **Comparison of the o2 loop sequences of the five human muscarinic receptor subtypes (M_1–M_5).** *Numbers* indicate M3R residues (*top row*) whose presence is required for efficient carbachol-induced M3R activation. Amino acid numbers refer to positions in the rat M3R sequence (46). Note that the rat and human M3Rs have identical sequences in the region displayed here. The *asterisks* indicate positions where all five muscarinic receptor subtypes have identical amino acids. Sequences were taken from Ref. 8.

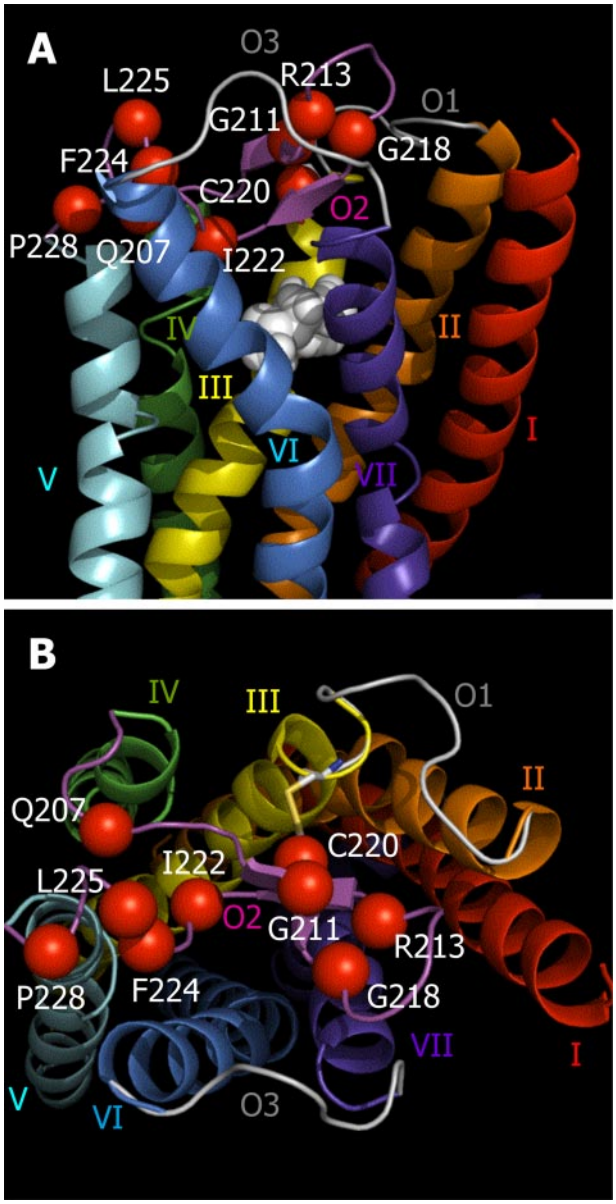

FIGURE 6. **Model of the inactive state of the M3R highlighting functionally critical amino acids in the o2 loop.** *A*, side view. *B*, extracellular view. The M3R model was established via homology modeling based on the crystal structure of the resting state of bovine rhodopsin (11, 48). The o2 loop (*magenta*) is predicted to fold deeply into the center of the receptor core. The second and third extracellular loops (o1 and o3, respectively), which are displayed as *white-gray bands*, are short and run along the periphery of the receptor. The extracellular N-terminal domain is not shown for the sake of clarity. Amino acids located in the o2 loop of the M3R whose presence is required for efficient carbachol-induced M3R activation are highlighted in *red* (C-α atoms). The *white* molecule present at the center of the receptor in *A* represents the endogenous ligand, acetylcholine, docked into its binding site within the TM receptor core. Amino acid numbers refer to positions in the full-length rat M3R sequence (46).

yeast genetic screen to recover mutant receptors that retained functional activity. Interestingly, the authors identified a series of mutant C5a receptors containing multiple point mutations in the o2 loop that were able to activate G proteins even in the absence of ligands. These findings led to the proposal that specific o2 loop residues establish contacts with the TM receptor core, thus stabilizing the inactive state of the receptor (26). However, by using random mutagenesis of the entire M3R coding sequence, followed by yeast genetic screens, we have been unable to identify activating point mutations in the o2 loop of the M3R.[4] Similarly, previous random mutagenesis studies carried out with the angiotensin II type 1A (39) and the δ-opioid (40) receptors failed to identify point mutations in the o2 loop that rendered these receptors constitutively active.

In contrast to the model proposed by Klco *et al.* (26), the results of this study rather suggest that specific o2 loop residues are required for efficient agonist-induced M3R activation. We found that amino acid substitutions at several specific sites within the o2 loop had pronounced effects on functional carbachol potencies but only minor effects on carbachol binding affinities. Therefore, one likely scenario is that the side chains of the mutated amino acids are involved in interactions that stabilize the active state of the M3R that can productively interact with G proteins. This concept is in agreement with the outcome of a previous study demonstrating that several o2 loop residues determine whether ATP functions as an agonist or an antagonist at mammalian $P2Y_4$ receptors (41). Moreover, Baneres *et al.* (42) recently provided direct biophysical evidence that agonist binding to the serotonin $5\text{-}HT_{4(a)}$ receptor is associated with a rearrangement of the o2 loop.

In contrast to the results that we obtained with the o2 loop library, our yeast genetic screen failed to recover any single inactivating point mutations located within the N-term region of the M3R (Thr^2–Gln^{66}). Transient expression of a mutant M3R lacking Thr^2–His^{62} led to an ~90% reduction in receptor expression levels (B_{max}), as compared with the "WT" M3R (Table 2). When the "WT" M3R was expressed at similarly low levels, carbachol was able to activate the two receptors with similar potencies and efficacies. These observations indicate that the N-term region of the M3R most likely plays a role in M3R stability and/or cell surface trafficking but does not contain structural elements that determine the efficiency of agonist-induced receptor activation. It is likely that this domain has a similar function in other class I GPCRs.

In the yeast genetic screen, we identified many mutant M3Rs that contained multiple point mutations within the N-term region. Therefore, one possibility is that these mutant M3Rs are functionally inactive in yeast because of reduced stability and/or impaired cell surface trafficking.

In conclusion, we used receptor random mutagenesis and a novel yeast genetic screen to identify inactivating point mutations located in the o2 loop of the M3R. Pharmacological characterization of many of the recovered mutant M3Rs in mammalian cells, complemented by site-directed mutagenesis studies, strongly suggested that the presence of several o2 loop residues is important for efficient agonist-induced M3R activation. Because mutational modification of these residues had little effect on agonist binding affinities, a likely scenario is that these residues stabilize the active state of the M3R.

To the best of our knowledge, this study represents the most comprehensive analysis of the functional role of the o2 loop of a class I GPCR activated by a small diffusible ligand. The approach described here should be applicable to all GPCRs that can be expressed in yeast in a functional form (43–45).

[4] B. Li, C. Schmidt, and J. Wess, unpublished results.

Acknowledgment—We thank Dr. Jean-Marc Guettier (NIDDK, National Institutes of Health) for critical reading of the manuscript.

REFERENCES

1. Bockaert, J., and Pin, J. P. (1999) *EMBO J.* **18,** 1723–1729
2. Gether, U. (2000) *Endocr. Rev.* **21,** 90–113
3. Pierce, K. L., Premont, R. T., and Lefkowitz, R. J. (2002) *Nat. Rev. Mol. Cell Biol.* **3,** 639–650
4. Fredriksson, R., Lagerström, M. C., Lundin, L.-G., and Schiöth, H. B. (2003) *Mol. Pharmacol.* **63,** 1256–1272
5. Kristiansen, K. (2004) *Pharmacol. Ther.* **103,** 21–80
6. Foord, S. M., Bonner, T. I., Neubig, R. R., Rosser, E. M., Pin, J. P., Davenport, A. P., Spedding, M., and Harmar, A. J. (2005) *Pharmacol. Rev.* **57,** 279–288
7. Strader, C. D., Fong, T. M., Tota, M. R., Underwood, D., and Dixon, R. A. (1994) *Annu. Rev. Biochem.* **63,** 101–132
8. Wess, J. (1996) *Crit. Rev. Neurobiol.* **10,** 69–99
9. Shi, L., and Javitch, J. A. (2002) *Annu. Rev. Pharmacol. Toxicol.* **42,** 437–467
10. Lu, Z. L., Saldanha, J. W., and Hulme, E. C. (2002) *Trends Pharmacol. Sci.* **23,** 140–146
11. Palczewski, K., Kumasaka, T., Hori, T., Behnke, C. A., Motoshima, H., Fox, B. A., Le Trong, I., Teller, D. C., Okada, T., Stenkamp, R. E., Yamamoto, M., and Miyano, M. (2000) *Science* **289,** 739–745
12. Zeng, F.-Y., Soldner, A., Schöneberg, T., and Wess, J. (1999) *J. Neurochem.* **72,** 2404–2414
13. Shi, L., and Javitch, J. A. (2004) *Proc. Natl. Acad. Sci. U. S. A.* **101,** 440–445
14. Karlsson, E., Jolkkonen, M., Mulugeta, E., Onali, P., and Adem, A. (2000) *Biochimie* (*Paris*) **82,** 793–806
15. Bradley, K. N. (2000) *Pharmacol. Ther.* **85,** 87–109
16. Kukkonen, A., Perakyla, M., Akerman, K. E., and Nasman, J. (2004) *J. Biol. Chem.* **279,** 50923–50929
17. Birdsall, N. J., and Lazareno, S. (2005) *Mini-Rev. Med. Chem.* **5,** 523–543
18. Li, B., Scarselli, M., Knudsen, C. D., Kim, S. K., Jacobson, K. A., McMillin, S. M., and Wess, J. (2007) *Nat. Meth.* **4,** 169–174
19. Stefan, C. J., and Blumer, K. J. (1994) *Mol. Cell. Biol.* **14,** 3339–3349
20. Konopka, J. B., Margarit, S. M., and Dube, P. (1996) *Proc. Natl. Acad. Sci. U. S. A.* **93,** 6764–6769
21. Sommers, C. M., and Dumont, M. E. (1997) *J. Mol. Biol.* **266,** 559–575
22. Baranski, T. J., Herzmark, P., Lichtarge, O., Gerber, B. O., Trueheart, J., Meng, E. C., Iiri, T., Sheikh, S. P., and Bourne, H. R. (1999) *J. Biol. Chem.* **274,** 15757–15765
23. Erlenbach, I., Kostenis, E., Schmidt, C., Serradeil-Le Gal, C., Raufaste, D., Dumont, M. E., Pausch, M. H., and Wess, J. (2001) *J. Biol. Chem.* **276,** 29382–29392
24. Schmidt, C., Li, B., Bloodworth, L., Erlenbach, I., Zeng, F. Y., and Wess, J. (2003) *J. Biol. Chem.* **278,** 30248–30260
25. Li, B., Nowak, N. M., Kim, S. K., Jacobson K. A., Bagheri, A., Schmidt, C., and Wess, J. (2005) *J. Biol. Chem.* **280,** 5664–5675
26. Klco, J. M., Wiegand, C. B., Narzinski, K., and Baranski, T. J. (2005) *Nat. Struct. Mol. Biol.* **12,** 320–336
27. Erlenbach, I., Kostenis, E., Schmidt, C., Hamdan, F. F., Pausch, M. H., and Wess, J. (2001) *J. Neurochem.* **77,** 1327–1337
28. Cadwell, R. C., and Joyce, G. F. (1994) *PCR Methods Applications* **3,** S136–S140
29. Oldenburg, K. R., Vo, K. T., Michaelis, S., and Paddon, C. (1997) *Nucleic Acids Res.* **25,** 451–452
30. Sommers, C. M., and Dumont, M. E. (1999) in *Structure-Function Analysis of G Protein-coupled Receptors* (Wess, J., ed) pp. 141–166, Wiley-Liss, Inc., New York
31. Behrendt, H. J., Germann, T., Gillen, C., Hatt, H., and Jostock, R. (2004) *Br. J. Pharmacol.* **141,** 737–745
32. Cheng, Y., and Prusoff, W. H. (1973) *Biochem. Pharmacol.* **22,** 3099–3108
33. Schöneberg, T., Liu, J., and Wess, J. (1995) *J. Biol. Chem.* **270,** 18000–18006
34. Maggio, R., Barbier, P., Fornai, F., and Corsini, G. U. (1996) *J. Biol. Chem.* **271,** 31055–31060
35. Ballesteros, J. A., and Weinstein, H. (1995) *Methods Neurosci.* **25,** 366–428
36. Kurtenbach, E., Curtis, C. A., Pedder, E. K., Aitken, A., Harris, A. C., and Hulme, E. C. (1990) *J. Biol. Chem.* **265,** 13702–13708
37. Ballesteros, J. A., Shi, L., and Javitch, J. A. (2001) *Mol. Pharmacol.* **60,** 1–19
38. Beukers, M. W., and Ijzerman, A. P. (2005) *Trends Pharmacol. Sci.* **26,** 533–539
39. Parnot, C., Bardin, S., Miserey-Lenkei, S., Guedin, D., Corvol, P., and Clauser, E. (2000) *Proc. Natl. Acad. Sci. U. S. A.* **97,** 7615–7620
40. Decaillot, F. M., Befort, K., Filliol, D., Yue, S., Walker, P., and Kieffer, B. L. (2003) *Nat. Struct. Biol.* **10,** 629–636
41. Herold, C. L., Qi, A. D., Harden, T. K., and Nicholas, R. A. (2004) *J. Biol. Chem.* **279,** 11456–11464
42. Baneres, J. L., Mesnier, D., Martin, A., Joubert, L., Dumuis, A., and Bockaert, J. (2005) *J. Biol. Chem.* **280,** 20253–20260
43. Pausch, M. H. (1997) *Trends Biotechnol.* **15,** 487–494
44. Dowell, S. J., and Brown, A. J. (2002) *Recept. Channels* **8,** 343–352
45. Minic, J., Sautel, M., Salesse, R., and Pajot-Augy, E. (2005) *Curr. Med. Chem.* **12,** 961–969
46. Bonner, T. I., Buckley, N. J., Young, A. C., and Brann, M. R. (1987) *Science* **237,** 527–532
47. Pausch, M. H., Price, L. A., Kajkowski, E. M., Strnad, J., dela Cruz, F., Heinrich, J., Ozenberger, B. A., and Hadcock, J. R. (1998) in *Identification and Expression of G Protein-coupled Receptors* (Lynch, K. R., ed) pp. 196–212. Wiley-Liss, Inc., New York
48. Han, S. J., Hamdan, F. F., Kim, S. K., Jacobson, K. A., Brichta, L., Bloodworth, L. M., Li, J. H., and Wess, J. (2005) *J. Biol. Chem.* **280,** 24870–24879